A Lower Limb EMG-driven Biomechanical Model for Applications in Rehabilitation Robotics

Massimo Sartori, Monica Reggiani, Cristiano Mezzato, Enrico Pagello

Abstract— **Current changes in aging demographics poses new challenges: people require to keep their quality of life even after circumstances that threatened their movement and function. This increases the demand for new physical rehabilitation facilities that go beyond the traditional patient-therapist, one-to-one rehabilitation sessions. Two promising solutions rely on virtual reality and on the development of autonomous active orthoses, or exoskeletons. Whatever is the chosen approach, there is a requirement for a robust human-machine interface for the control, able to understand patient's intention and to produce an immediate activation of the device.**

This paper presents a biomechanical model, a possible solution able to predict joint torque from the surface electromyography signals emitted by muscles during their activation. The main objective of the research is to investigate the benefits and efficacy of this model and to lay down the basis of our current research, whose main goal is to make possible a rehabilitation process either with active orthoses or virtual reality. Experiments involving all the steps of our model demonstrate the viability and effectiveness of our approach.

I. INTRODUCTION

Aging societies pose new challenges, creating new needs and aspirations. People desire to have a high quality of life and the possibility to easily create social interactions even after circumstances that threatened their movement and function, such as aging, injury, disease or environmental factors. To restore movement and functional abilities it is central the possibility to have access to physical rehabilitation facilities, which are quite expensive as they still continuously require the knowledge and skills of a physical therapist.

Research is currently looking for alternative solutions, mainly in the fields of virtual reality [1] and autonomous active orthoses [2]. Virtual reality (VR) technologies have the potential to become of primarily importance in rehabilitation, due to the several strengths underlying its use. The main advantage is the availability of a controlled environment, where the user's feedback and the training can be manipulated based on patient conditions to create a personalized rehabilitation experience. Furthermore, doing exercises in VR helps motivation, augmenting the operator's attention [3].

Another research opportunity is the integration of human and exoskeleton or orthoses to develop a new generation of assisting technologies [2]. With respect to rehabilitation, the goal is to have active technologies, still under the final control of the user, to both support, amplifying human movement, and rehabilitate through active training.

Whatever the chosen research approach is, there is a need of an interface between the patient and the real or virtual device: as soon as the patient's intention is raised, the interface should activate, accordingly, the device. A possible, promising solution utilizes surface electromyography (EMG) signals emitted by muscles during their activation. During the execution of the movement, these signals are interpreted and used as input for the control algorithms. Together with a simple user interface (the execution of the movement) EMG signals have another advantage, i.e. a delay between the activation and the actual movement. This time delay, usually in the range of 26-131 ms [4], can be used to provide a run-time actuation for the supporting device.

The main problem with surface EMG signals is that they are not stationary and not linear, therefore they require the development of a sophisticated model for their interpretation. Promising and complete models are already available in literature [5], [6] but their complexity relegate them to offline computation. Proposed models, running within the EMG electromechanical delay, are often based on classification algorithms. Only recently, few researchers have developed biologically-motivated models [7], [8]. In [9], the authors present a model of the human muscle able to predict joint torques for the upper limb as a function of the joint kinematics and neural activation level. Another effective research has been presented in [10]. The EMG signals are used as input for a simplified biomechanical model able to derive the desired action of the operator and control an orthoses for the knee joint.

Starting from this research, we present a biomechanical model based on EMG signals we have developed for the control of lower limb devices. Although the potential benefits of rehabilitation for both upper and lower extremity, we have decided to focus our efforts on the human leg because of the lack of research when compared with the advancements on upper extremity exoskeletons. While the latter have been studied for more than ten years, only recently particular attention has been put on lower extremity exoskeletons and human gait support despite the potentially large number of consumers [10]–[13].

The model is at the basis of our current research, whose main goal is to make possible the analysis and immediate feedback to subjects, and physical therapists, to support rehabilitation processes either in VR or through active or-

M. Sartori and E. Pagello are with the Department of Information Engineering, University of Padova and with the Institute of Biomedical Engineering - National Research Council, Padova, Italy. massimo.sartori@dei.unipd.it,

M. Reggiani is with the Department of Technique and Management, University of Padova, Vicenza, Italy,

C. Mezzato is with the Department of Information Engineering, University of Padova, Padova, Italy.

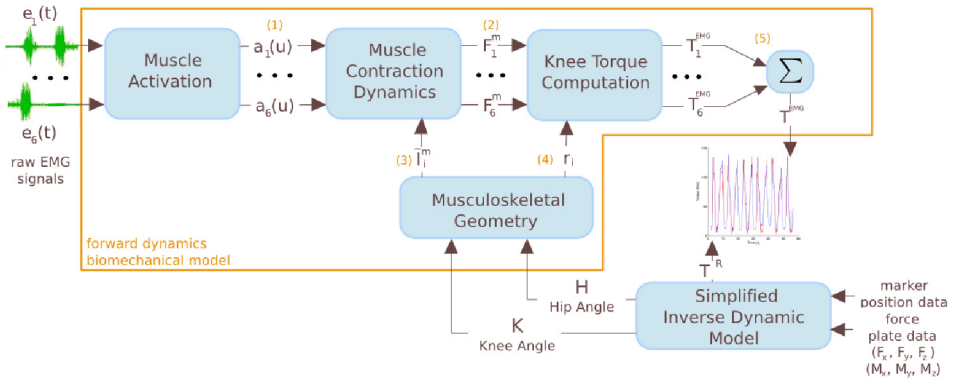

Fig. 1: A forward dynamic approach has been used to estimate the subject's movements starting from the muscle activity. An inverse dynamic approach has been used to obtain reference values for angles and torques.

thoses. To cope with the application requirements, our model has to provide a good balance between complexity, and therefore accuracy, and efficiency, to operate within the short delay allowed by EMG signals. Details about the proposed biomechanical model to estimate muscle forces and joints moment for the knee articulation are presented in Section II.

Physiological models require an additional step to be effective: the calibration of some parameters related to EMGs signals and musculoskeletal geometry. Those parameters show a large variance not only between different users but also on patient's conditions thus requiring a new calibration before every rehabilitation session. Section III describes the two implemented solutions: the first one based on isometric conditions while the second one works on data gathered from an operator executing a sit-to-stand movement. Section V reports some experiments involving the whole steps of our model demonstrating the viability and effectiveness of the approach.

II. MODEL STRUCTURE

This section describes our proposal for a biologically-motivated model (Fig. 1). It combines together results of previous promising research in biomechanical modeling [6], [9], [10], [14]. We introduced some simplifications w.r.t. complex models to cope with performance requirements while retaining the required accuracy as demonstrated in Sec. V. The inputs for our *forward dynamics EMG-driven biomechanical model* include the raw EMG signals ($e(t)$), and both hip (H) and knee (K) joint angles (Fig. 1). The model is then able to estimate individual muscle forces (F^m) and knee joint moments (T^{EMG}) during the analyzed movements.

To validate the prediction accuracy of the EMG-driven model, we compared the estimated joint torque towards the reference torque, (T_R) obtained from an inverse dynamic model (Fig. 1). Within the error associated with inverse dynamic methods, we were able to cross-validate the accuracy prediction of our model (Sec. V).

For the purpose of this study, we concentrated on the knee joint. However, the model can be easily adapted to any articulation. This can be done by including in the *musculoskeletal geometry model* (Sec. II-A.3) anatomical data regarding the muscles that span the joint to be added. Muscle anatomical data includes: origin and insertion points and via points that appear when the individual muscle wraps around bones depending on the angle of the joints the muscle spans. This approach is well described by Delp *et* al. in [15]. Furthermore, a complete knee model would require measurements from all muscles that span the knee articulation. Our inputs were, instead, reduced to a meaningful subset of the muscles that surface electrmyography techniques can measure. We therefore selected six muscles depending on their physiological cross-sectional area (PCA) and proximity to the skin surface [10]. Among the flexors we selected: rectus femoris, vastus medialis, vastus lateralis. Among the extensors we chose: biceps femoris, semitendinosus, semimembranosus.

A. Forward Dynamics EMG-driven Biomechanical Model

The logical blocks that allow to move from the neural command (EMG) to the evaluation of individual muscle forces and joint moments are described in the following.

1) Muscle Activation Model: Its purpose is to represent the level of active force produced by a muscle relative to its maximum voluntary contraction (MVC). For every muscle i, the corresponding raw EMG $e_i(t)$ is postprocessed to obtain the activation envelope $u_i(t)$. Due to lack of space we omitted a complete description of the EMG signal post processing stage and refer the reader to the work done by Buchanan *et* al. [16]. The muscle activation can then be computed as: $a_i(u_i) = \frac{e^{A_i u_i R_i^{-1}} - 1}{e^{A_i} - 1}$, where u_i is the postprocessed EMG signal, A_i is the non-linear shape factor constrained to $-5 < A_i < 0$, with 0 being a linear relationship and R_i is the peak rectified EMG value obtained during MVC.

2) Muscle Contraction Dynamics: For the muscle i, muscle-tendon length l_i^{mt}, together with activation data $a_i(u_i)$, are used as input to a modified Hill-type muscle model [5] to calculate muscle forces:

$$F_i^m = ((f_{Ai}(\tilde{l}_i^m))a_i(u_i) + (f_{Pi}(\tilde{l}_i^m)))F_{0i}^m \qquad (1)$$

where $f_{Ai}(\tilde{l}_i^m)$ and $f_{Pi}(\tilde{l}_i^m)$ are the active and passive force length curves as a function of the normalized muscle fiber length $\tilde{l}_i^m$. This last quantity is normalized with respect to the optimal muscle fiber length, l_{0i}^m which is the length at which the muscle produces maximal force, *i.e.*, $\tilde{l}_i^m = \frac{l_i^m}{l_{0i}^m}$. Finally, F_{0i}^m denotes the maximum muscle force at optimal fiber length.

3) Musculoskeletal Geometry: A lower limb anatomical model was created based on the model proposed by S.L. Delp [17] and extended by Lloyd and Buchanan [14]. The muscles selected for this study are represented as line segments that wrap around bones and other muscles depending on the hip and knee angle. Lower limb joint kinematics data (hip and knee joint angles) is used as input. The geometry model is then able to determine individual muscle-tendon lengths l_i^{mt} and muscle fibers length l_i^m (Fig. 1).

We assumed the tendon is stiff and the muscle-tendon length change is only due to muscle fibers. Normalized fiber length can then be computed with respect to the tendon length:

$$\tilde{l}_i^m = \frac{l_i^{mt} - s_i^t \hat{l}_{si}^t}{s_i^t \hat{l}_{si}^t} \tag{2}$$

where $\hat{l}_{si}^t$ is the tendon slack length for the i-th muscle according to literature. This quantity defines the length of the tendon when no tension is applied. From our assumptions on tendon stiffness it follows that the length of the tendon can be approximated with $\hat{l}_{si}^t$. Parameter s_i^t represents the tendon slack length scale and plays an important role for tuning the model to the actual subject's musculoskeletal geometry.

Muscle moment arms are also computed by the model as a function of the joint angle θ:

$$r_i(\theta) = \frac{\partial l_i^{mt}(\theta)}{\partial \theta} \tag{3}$$

For biarticular muscles (muscles that cross two joints) such as rectus femoris and all the flexor muscles included in our model, the moment arm is a function of both hip and knee angles. Muscle moment arms are really important in the model as they influence a great number of factors including: the estimated torque resulting at the knee joint and the individual muscle forces computed by solving the *force sharing problem* (Sec. II-A.4 and IV-A.3).

4) Joint Torque Computation: Performing the previous computations for every muscle i with $1 < i < N$ yields for the resulting knee torque: $T^{EMG} = \sum_{i=1}^{N} r_i F_i^m$, where $r_i F_i^m$ represents the individual torque generated by the muscle i, (T_i^{EMG}).

III. PARAMETERS SELECTION

Several parameters characterize the proposed model. They have to be properly adjusted to assure adaptation to the current subject's anatomical structure and physiological condition. The more parameters are allowed to vary, the better the fit between the estimated joint torque and the measured one will be. However, models that have many parameters provide highly accurate prediction only within a few time steps with the need of reevaluate them at each time instant [16]. Therefore, parameters to calibrate have to be accurately selected. Furthermore, the number of parameters that are allowed to vary, strongly influences the number of sensors the model needs. For the design of a highly predictive system that can also be easily applied to any subject with reasonable preparation time this number has to be kept low.

For each muscle i, we selected the following parameters: (1) maximal muscle force at optimal fiber length, $F_{0,i}^m$, (2) EMG-to-Force shape factor, A_i, (3) tendon slack length scale, s_i^t. The last one is only related to the musculoskeletal geometry, therefore it is a constant for the human being and requires to be calibrated only once for every operator. The remaining parameters are highly *EMG-dependent* and need to be re-calibrated at each experimental session for optimal performances. All factors that are out of this list and that are not derived from the formulas presented in this paper are taken directly from literature.

IV. CALIBRATION

We implemented two different types of calibration. The first one (*Isometric Calibration*) involves only isometric trials. This procedure was proved to be quite laborious in terms of subject's preparation and instrumentation setup. Furthermore, muscles such as vastus lateralis and vastus medialis did not show significant activity. Therefore, we conceived an alternative approach (*Dynamic Calibration*) based on a more intuitive and faster procedure suitable for dynamic movements. This way we assured a greater activity of the vasti.

A. Isometric Calibration

The reference values for the isometric calibration are the knee angle and torque measured during isometric contractions. It is noteworthy pointing out that the following procedure is completely general and can be applied to any joint. This statement follows by the fact that we adopted the general calibration approach described in [10].

1) Calibration Setup: The operator is sitting on a chair with the thigh comfortably supported and the shank secured into a special structure (*MVC-structure*) to avoid any knee flexo-extension movements. The structure is designed to touch the ground only in four points (Fig. 2) and to avoid any contact between the subject's leg and the floor.

The knee can be secured at any arbitrary angle whereas the hip is kept at 90° (Fig. 2-a). Both pelvis and thigh are strapped up to the chair so that no undesired movements can occur during the calibration procedure. The MVC-structure is placed above two force plates that measure only the weight of the leg and of the blocking structure when the muscles are relaxed. In the correspondence of such a weight, the force plates are set to measure $0N$.

During each trial the operator is asked to extend or flex the knee with maximum force. The static equilibrium of the system (MVC-structure and leg) allows to derive the torque at the knee joint. Depending on the nature of the movement (flexion or extension), two opposite forces are generated

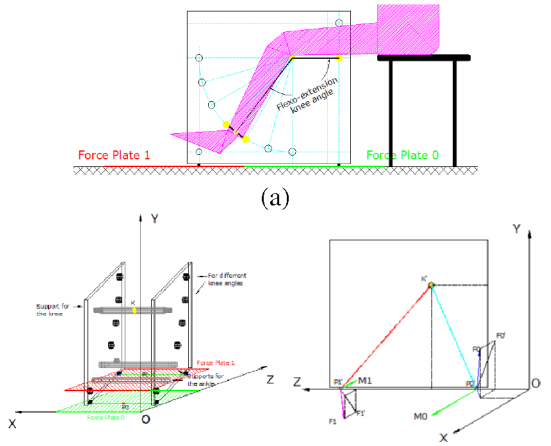

Fig. 2: (a) Setup for the isometric calibration. (b) A 3D sketch of the structure is shown. Moment arms for the forces $F0$ and $F1$ measured on the force plates are computed with respect to the lines of action from the point K to the contact points $P0$ and $P1$, respectively. The projection of 3D points and forces on the zy-plane are indicated as: K',$F'0$, $F'1$, $P'0$, $P'1$.

orthogonally to the xz-plane on the two force plates. Moment arms for both forces are computed at each instant of time and the torque exerted at the knee is therefore measurable. In the following a knee angle of $0°$ represents a straight leg and negative angles indicate knee flexion. Three isometric flexion trials were performed at $-44°$, $-42°$, and $-51°$ while four isometric extension trials took place at $-33°$, $-34°$, $-41°$, and $-67°$.

2) Data Selection and Storage: During each trial, we measure the EMG signals of all six selected muscles, the knee and hip angles, and the torque at the knee. Data selection follows the approach presented in [10]. For each trial k ($1 \leq k \leq K$), a table is created for each muscle i included in the model. The postprocessed EMG signal $u_{k,i}$ linearly maps to a specific entry $h_{k,i}$ as follows: $h_{k,i} = \lfloor u_{k,i} S \rfloor$, where S is the entry width ($0.0025mV$ in our calibration procedure). Every entry contains one value for every recorded quantity, and is averaged with new values whenever the table entry is selected for storing new data. At the end of this process every muscle owns K tables, one for each trial.

3) Force Sharing Problem: The reference joint torque T_R is distributed among all muscles according to their activation. This allows to calibrate the geometry parameters related to every individual muscle separately. To predict the load sharing of synergistic muscles we adopted the approach introduced in [18]. The force share, $F^m_{R,i}$, for the i-th muscle is calculated based on T_R, as follow:

$$F^m_{R,i} = \begin{cases} \dfrac{T_R}{\sum_{j \in group} r_j (\frac{r_j}{r_i})^{1/2} (\frac{PCA_j}{PCA_i})^{3/2}} & i,j \text{ out of same group} \end{cases} \quad (4)$$

where PCA_i is the physiological cross sectional area of muscle i and its value is taken from the literature [10]. Muscles with a larger cross sectional area are given a higher force share depending also on their moment arms. Predictions are sensibly improved when moment arms vary with respect to the joint angle as implemented in our study. The term *group* represents either the group of extensors or flexor muscles.

4) Geometry Calibration (s^t): After the force sharing computation, the tables associated to each muscle are updated. The data stored in the entry $h_{k,i}$ is now:

$u_{h_{k,i}}$	$K_{h_{k,i}}$	$H_{h_{k,i}}$	$F^m_{R,h_{k,i}}$	na

where na is the number of updates. The goal of the geometry calibration is to optimize the tendon slack length scale (s^t) for every muscle. We followed the approach described in [10]. For the muscle i, the muscle activation for the entry $h_{k,i}$ is computed solving Eq. 1 for $a(u)$:

$$a_{h_{k,i}} = \frac{\frac{F^m_{R,h_{k,i}}}{F^m_{0i}} - f_{Pi}(\tilde{l}^m_i)}{f_{Ai}(\tilde{l}^m_i)} \quad (5)$$

This equation depends on s^t_i that is incorporated in $\tilde{l}^m_i$ (Eq. 2). The standard deviation, which is a function of s^t_i, is then computed for a particular entry h among all K trials for the muscle i as: $\sigma_h(s^t_i) = \sqrt{\frac{1}{K}\sum_{k=1}^{K}(a_{h_{k,i}} - \overline{a}_{h,i})^2}$, where $\overline{a}_{h,i}$ is the average of $a_{h_{k,i}}$ over all trials. The scale s^t_i can now be optimized by minimizing the average of all standard deviations for every entry h:

$$min_{s^t_i}(\overline{\sigma}(s^t_i)) = min_{s^t_i}\left(\frac{1}{N_h}\sum_{h=1}^{N_h}(\sigma_h(s^t_i))\right) \quad (6)$$

where N_h is the number of entries in the tables. The optimization is then performed by varying the scale s^t_i in the interval $[0.85, 1.25]$ with a fixed step size of 0.01. A subspace search algorithm is used. As long as F^m_0 is not known from previous calibrations, its value is replaced with the one available in literature [15].

Fig. 3 a-d show the effect of the geometry calibration on an extensor muscle (vastus lateralis) and on a flexor muscle (biceps femoris). When s^t is not calibrated the muscle activation function assumes different values at different angles for the same level of normalized postprocessed EMG, $\tilde{u} = \frac{u}{R}$. After s^t is calibrated the muscle activation has a close behavior for different trials. Fig. 3 e-h show another important effect on another couple of extensor and flexor muscles (vastus medialis and semitendinosus), pointing out the importance of s^t. Before the calibration, the muscle force estimated by the model assumes highly different trends for the same level of $\tilde{u}$ over the different trials. After the calibration, the force exerted by the muscle for a certain value of $\tilde{u}$ is always the same regardless of: (1) the knee angle when flexed and (2) the current muscle-tendon length. This demonstrates the importance of the *force length curve* for a correct muscle force estimation (Eq. 1).

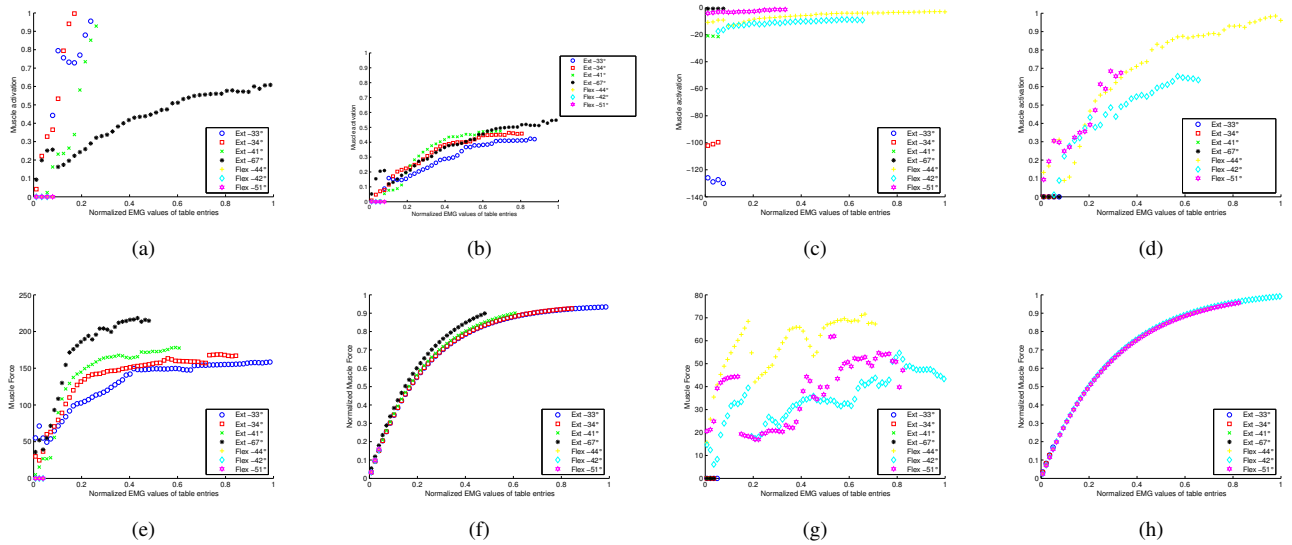

Fig. 3: Muscle activation functions behave differently for the same level of $\tilde{u}$ over different trials (angles) when s^t is not calibrated: (a) vastus lateralis (s^t not calibrated), (b) vastus lateralis (s^t calibrated), (c) biceps femoris (s^t not calibrated), (d) biceps femoris (s^t calibrated). The muscle force behaviour after calibration is consistent with respect to the same level of $\tilde{u}$: (e) vastus medialis (s^t not calibrated), (f) vastus medialis (s^t calibrated), (g) semitendinosus (s^t not calibrated), (h) semitendinosus (s^t calibrated).

5) EMG-to-Force Calibration (F_0^m, A): The optimized EMG-dependent parameters F_0^m and A are computed by curve fitting the trend of the muscle force F_R^m computed from Eq. 4 for all muscles and trials. The error function to be optimized for the i-th muscle is:

$$E_i(F_{0i}^m, A_i) = \sum_{k=1}^{K} \sum_{h=1}^{N_h} \left(\widehat{F}_{h_{k,i}}^m - F_{R,h_{k,i}}^m \right)^2 \qquad (7)$$

where $\widehat{F}_{h_{k,i}}^m$ is calculated from Eq. 1. We assumed that $-5 < A < 0$ and $100N < F_0^m < 2500N$, [15]. After the EMG-parameter calibration is done, the geometry calibration is performed once again using the optimized value F_0^m to refine the torque estimation. Figure 4 shows the optimization function correctly fitting the *geometry-calibrated* muscle activation-force relationship (also see Eq. 7 and 1).

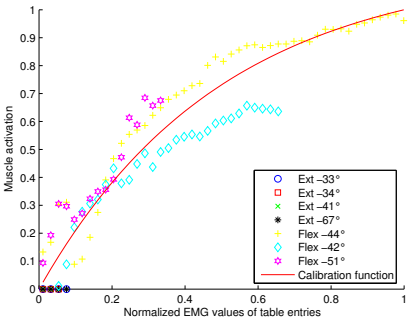

Fig. 4: Parameters A and F_0^m are tuned to have the best fit of the optimization function with respect to the calibrated activation-force relationship (Eq. 5). The other muscles show behavior similar to the one shown for the biceps femoris.

B. Dynamic Calibration

The dynamic calibration procedure has been applied to sit-to-stand movements.

The subject is initially sitting on a chair with both feet on a ground force plate and has to slowly get up from the chair without supporting himself with his hands. A set of markers are placed on the pelvis and on the right leg so that the limb trajectories in the sagittal plane can be determined (Fig. 5-a). Reference values for hip and knee angles (H, K) and knee torque (T_R) are derived from an inverse dynamic model we implemented using the Smart Analyzer software [19]. The model is developed according to the one presented in [20]. The kinematics data is derived from 3D marker positions while joint angles and force values on the force plates allow to compute the torques at each joint. This is a recursive process that starts from the computation of the ankle torque and continues upwards with the calculation of the knee and hip joint torques (Fig. 5-b). Only A and F_0^m are tuned for all muscles while the geometry parameter s^t is not included. In dynamic conditions it is difficult indeed to apply the optimization based on Eq. 6. The reason is that we need to minimize the discrepancy between the level of muscle activation, relative to a certain normalized EMG value, for different angles. This can be easily done by performing several isometric trials for different angles as explained in section IV-A.4. Dynamic movements do not allow to observe the muscle activation trend at a specific angle for different values of normalized EMG. Further research may

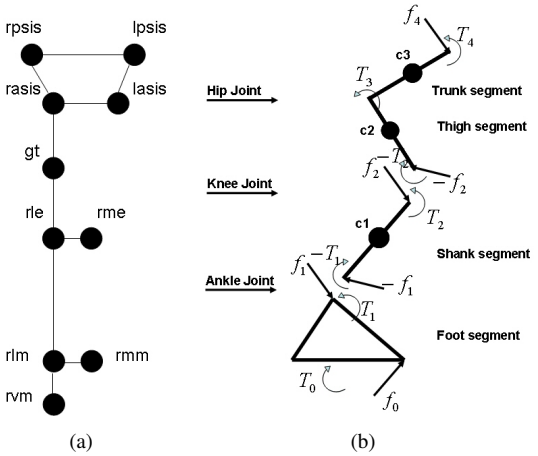

(a) (b)

Fig. 5: (a) Set of the anatomical points on the human lower limb where the markers are placed. (b) Schematic view of the inverse dynamic algorithm. Initial values of the ground force f_0 and the associated torque T_0 allow the computation of the ankle torque. Iteratively knee and hip torques are derived.

help understand how to get such information in dynamic conditions. A curve fitting with the data computed by the inverse dynamic model is performed for the calibration of the EMG-dependent parameters: $E(F_0^m, A) = \sum_j \left(T_{R,j} - T_j^{EMG}\right)^2$, where T_j^{EMG} is the torque estimated from the EMG-driven biomechanical model for the j-th muscle. Although, s^t could have been included in the curve fitting equation we preferred to avoid it. The inclusion of a further parameter would have decreased the prediction capacity of our model making it dependable on too many factors [16]. Experiments showed that our model has been able to correctly predict new sit-to-stand movements over a large amount of time. Since s^t has to be calibrated only once for a specific subject, we used the values we obtained from the isometric calibration. When such data was not available we used the ones taken from literature [15].

V. EXPERIMENTS

The experiments were performed at the Gait Analysis Laboratory of the Department of Information Engineering (University of Padova) on a 27 year old male subject with 1.83m height and 75Kg weight. A 6-camera motion track system and two force plates [19] were used to collect joint angles, ground forces and joint torques. A multichannel EMG acquisition system, equipped with wireless disposable bipolar electrodes, was used for the acquisition of the neural command. Angle data was sampled at $60Hz$ whereas torques and force data was sampled at $960Hz$. EMG signals were sampled at $1kHz$. All data was initially low pass filtered with a second order Butterworth filter with a cut off frequency of $6Hz$. The EMG-signals were further processed according to the procedure described in Sec. II-A.

This section provides evidence of the capability of our model to correctly predict knee joint moments in both isometric and dynamic conditions. The experiments also prove

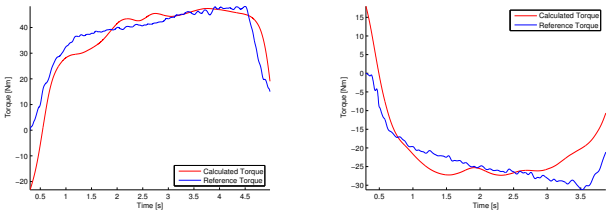

(a) (b)

Fig. 6: The estimated knee torque is superimposed to the measured one. (a) Isometric extension trial at $-67°$. (b) Isometric flexion trial at $-44°$.

the proper model behavior in dealing with new data, not used during calibration.

A. Isometric Trials

Isometric calibration was performed on the 7 trials listed in Sec. IV-A. We then ran the model with the optimized parameters on data from each trial. Fig. 6 shows the behavior of the system on two single tests. Our EMG-driven model correctly estimated the torque generated at the knee and produced a signal that resembled the reference one throughout the experiments. Some discrepancies between reference and simulated torques were however observable. Those were certainly due to the approach we used for measuring the reference knee torque (Fig. 2). More precisely, the moment arm for the ground forces, $F0$ and $F1$ were computed with respect to the lines of action that go from the point K to the contact points $P0$ and $P1$ (Fig. 2). Those lines of action, however, might not always be necessarily related to the forces $F0$ and $F1$. Furthermore, the subject's thigh was found to be always applying an undesired force on the plate $P0$. This fact introduced an additional external force that was not modeled.

B. Sit-to-Stand Movement

Calibration was performed on a complete sit-to-stand movement of the duration of approximately five seconds. Data was collected following the approach adopted for the isometric calibration (Sec. IV-A.2). Data collection procedure starts when the subject does not touch the chair anymore, at a knee extension of approximately $10°$. This ensures that there is no alteration on the measured torque due to undesired external forces. After optimized values for A and F_0^m are obtained for every muscle, a new session of data collection is performed on a new trial of 60 seconds including eleven sit-to-stand movements. The collected data is fed into the EMG-driven biomechanical model and the estimated EMG-based knee torque is compared with the one measured by the inverse dynamic system. Fig. 7-a shows good correlation of the data between the reference torque and the one estimated by our model. Fig. 7-b shows that the importance of the geometry parameter (s_t) for the estimation accuracy. The low correlation between reference and estimated data is clear. Fig. 7-c demonstrates the capability

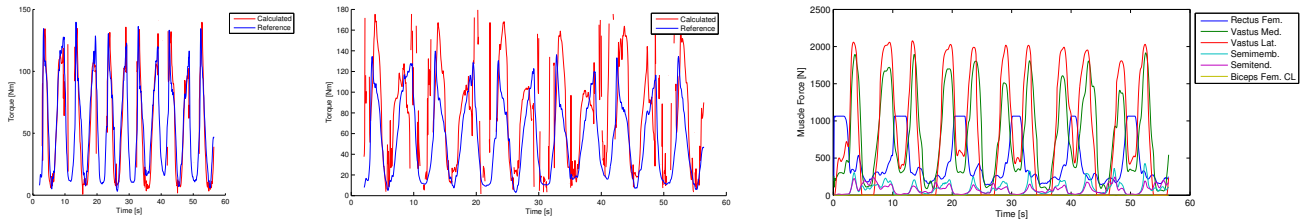

(a) (b) (c)

Fig. 7: Reference knee torque is compared with the estimated one: (a) s^t obtained from isometric calibration, (b) s^t not calibrated, (c) estimated muscle forces (s^t from isometric calibration).

of our model to estimate individual muscle forces. As we expected, the contribution of the vasti was predominant at the knee joint. The remaining muscles are biarticular and therefore distributed their contributions more uniformly between hip and knee. Flexor muscles were only active with low intensity.

VI. CONCLUSIONS AND FUTURE WORK

This paper proposed a biologically-motivated model to estimate knee torque from EMG signals in both isometric and dynamic conditions. Attention has been also devoted to the run time performance of the current implementation which is able to execute within the limit of time allowed by EMG electromechanical delay. The study has also shown the influence of the calibration process of muscoskeletal and EMG-dependent parameters on the prediction capabilities of the model. Finally, we demonstrated that reducing the calibration to an optimized subset of all the possible parameters can still result in an accurate model while reducing the execution time.

In our future work, we are planning to focus on the improvement of the dynamic calibration of parameters. This calibration of the whole set of chosen parameters, including s^t will allow the exoskeleton or VR model to continuously adapt to the varying conditions of user and EMG sensors. In the meanwhile, we have already started the integration of the model in the control of active orthoses and a VR model already developed in a previous research [21].

VII. ACKNOWLEDGMENTS

We would like to thank the members of the Gait Analysis Laboratory for their help and suggestions in collecting motion data. We would also like to thank the anonymous reviewers for their helpful comments.

REFERENCES

[1] "Intl. Society for Virtual Rehabilitation(ISVR)," http://www.isvr.org.

[2] A. M. Dollar and H. Herr, "Lower extremity exoskeletons and active orthoses: Challenges and state-of-the-art," *Robotics, IEEE Trans. on*, vol. 24, no. 1, pp. 144–158, 2008.

[3] V. Popescu, G. Burdea, M. Bouzit, and V. Hentz, "A virtual-reality-based telerehabilitation system with force feedback," *Information Technology in Biomedicine, IEEE Trans. on*, vol. 4, no. 1, pp. 45–51, 2000.

[4] P. Cavanagh and P. Komi, "Electromechanical delay in human skeletal muscle under concentric and eccentric contractions," *European Journal of Applied Physiology*, vol. 42, no. 3, pp. 159–163, 1979.

[5] D. G. Lloyd and T. F. Besier, "An EMG-driven musculoskeletal model to estimate muscle forces and knee joint moments in vivo," *Journal of Biomechanics*, vol. 36, no. 6, pp. 765–776, 2003.

[6] Y. Nakamura, K. Yamane, Y. Fujita, and I. Suzuki, "Somatosensory computation for man-machine interface from motion-capture data and musculoskeletal human model," *Robotics, IEEE Trans. on*, vol. 21, no. 1, pp. 58–66, 2005.

[7] H. Kawamoto and Y. Sankai, "Comfortable power assist control method for walking aid by hal-3," Oct. 2002.

[8] D. P. Ferris, K. E. Gordon, G. S. Sawicki, and A. Peethambaran, "An improved powered ankle-foot orthosis using proportional myoelectric control," *Gait Posture*, vol. 23, no. 4, pp. 425–428, 2006.

[9] E. Cavallaro, J. Rosen, J. Perry, and S. Burns, "Real-time myoprocessors for a neural controlled powered exoskeleton arm," *Biomedical Engineering, IEEE Trans. on*, vol. 53, no. 11, pp. 2387–2396, 2006.

[10] C. Fleischer and G. Hommel, "A human-exoskeleton interface utilizing electromyography," *Robotics, IEEE Trans. on*, vol. 24, no. 4, pp. 872–882, 2008.

[11] J. E. Pratt, S. H. Collins, B. T. Krupp, and K. J. Morse, "The RoboKnee: An Exoskeleton for Enhancing Strength and Endurance During Walking," in *IEEE Intl. Conf. on Robotics and Automation*, 2004.

[12] T. Hayashi, H. Kawamoto, and Y. Sankai, " Control Method of Robot Suit HAL working as Operators Muscle using Biological and Dynamical Information," in *IEEE Intl. Conf. on Systems, Man, and Cybernetics*, 2005.

[13] X. Low, K. H. Liu and H. Yu, "Development of NTU Wearable Exoskeleton System for Assistive Technologies," in *IEEE Intl. Conf. on Mechatronics and Automation*, 2005.

[14] T. S. Buchanan, D. G. Lloyd, K. Manal, and T. F. Besier, "Estimation of Muscle Forces and Joint Moments Using a Forward-Inverse Dynamics Model," *Medicine & Science in Sports & Exercise*, vol. 37, no. 11, pp. 1911–1916, 2005.

[15] S. Delp, F. Anderson, A. Arnold, P. Loan, A. Habib, C. John, E. Guendelman, and D. Thelen, "Opensim: Open-source software to create and analyze dynamic simulations of movement," *Biomedical Engineering, IEEE Trans. on*, vol. 54, no. 11, pp. 1940–1950, Nov. 2007.

[16] T. Buchanan, D. G. Lloyd, K. Manal, and T. Besier, "Neuromusculoskeletal modeling: Estimation of muscle forces and joint moments and movements from measurements from neural command," *Journal of Applied Biomechanics*, vol. 20, pp. 367–395, 2004.

[17] S. L. Delp, "Surgery Simulation: A Computer Graphics System to Analyze and Design Musculoskeletal Reconstructions of the Lower Limb," Ph.D. dissertation, Stanford University, 1990.

[18] R. D. Crownshield and R. A. Brand, "A physiologically based criterion of muscle force prediction in locomotion," *J. Biomech.*, vol. 14, no. 11, pp. 793–801, 1981.

[19] "BTS Bioengineering, Padova, Italy," http://www.isvr.org.

[20] A. Leardini, Z. Sawacha, G. Paolini, S. Ingrosso, R. Nativo, and M. G. Benedetti, "A new anatomically based protocol for gait analysis in children," *Gait Posture*, vol. 4, no. 26, pp. 560–571, 2007.

[21] M. Sartori, G. Chemello, M. Reggiani, and E. Pagello, "Control of a Virtual Leg via EMG Signals from Four Thigh Muscles," in *10th Intl. Conf. on Intel. Autonomous Systems*, 2008.